2015

Chronic optogenetic activation augments Aβ pathology in a mouse model of Alzheimer disease

Kaoru Yamamoto
The University of Tokyo

Zen-ichi Tanei
The University of Tokyo

Tadafumi Hashimoto
The University of Tokyo

Tomoko Wakabayashi
The University of Tokyo

Hiroyuki Okuno
The University of Tokyo

See next page for additional authors

Authors
Kaoru Yamamoto, Zen-ichi Tanei, Tadafumi Hashimoto, Tomoko Wakabayashi, Hiroyuki Okuno, Yasushi Naka, Ofer Yizher, Lief E. Fenno, Masashi Fukayama, Haruhiko Bito, John R. Cirrito, David M. Holtzman, Karl Deisseroth, and Takeshi Iwatsubo

Report

Cell Reports

Chronic Optogenetic Activation Augments Aβ Pathology in a Mouse Model of Alzheimer Disease

Graphical Abstract

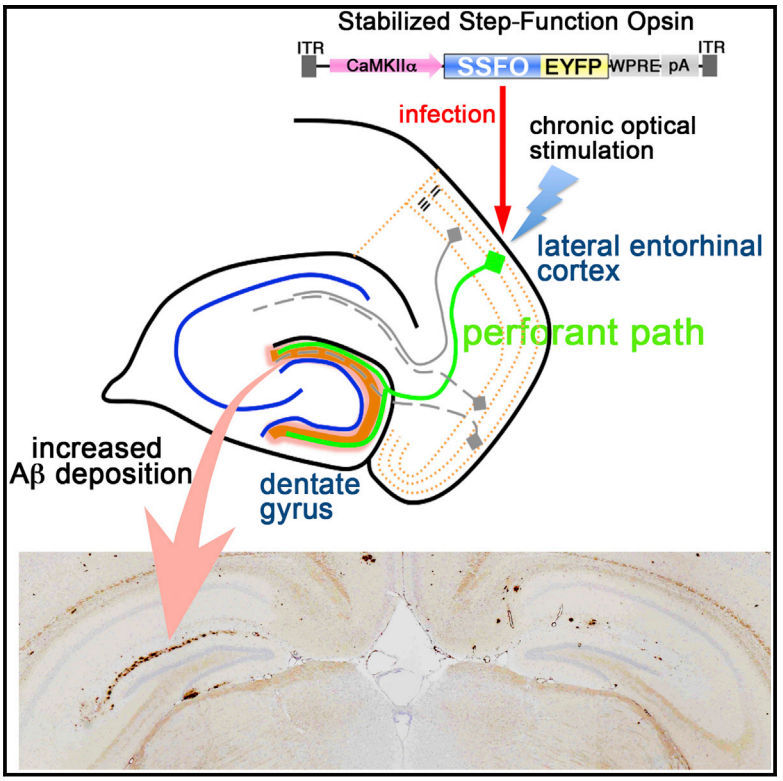

Authors

Kaoru Yamamoto, Zen-ichi Tanei, ..., Karl Deisseroth, Takeshi Iwatsubo

Correspondence

iwatsubo@m.u-tokyo.ac.jp

In Brief

Neuronal or synaptic activity has been implicated in the pathogenesis of Alzheimer disease. Yamamoto et al. show that chronic activation of the hippocampal perforant pathway in APP transgenic mice, using optogenetics, augments Aβ pathology within the presynaptic projection area in the dentate gyrus of the hippocampus.

Highlights

- Perforant pathway is chronically activated with stabilized step-function opsin
- Acute optogenetic activation increases the interstitial fluid Aβ42 level
- Five months of chronic activation increases Aβ deposition in the projection area

Yamamoto et al., 2015, Cell Reports *11*, 859–865
May 12, 2015 ©2015 The Authors
http://dx.doi.org/10.1016/j.celrep.2015.04.017

Cell Reports
Report

Chronic Optogenetic Activation Augments Aβ Pathology in a Mouse Model of Alzheimer Disease

Kaoru Yamamoto,[1,6] Zen-ichi Tanei,[1,2,6] Tadafumi Hashimoto,[1] Tomoko Wakabayashi,[1] Hiroyuki Okuno,[3] Yasushi Naka,[1] Ofer Yizhar,[4] Lief E. Fenno,[4] Masashi Fukayama,[2] Haruhiko Bito,[3] John R. Cirrito,[5] David M. Holtzman,[5] Karl Deisseroth,[4] and Takeshi Iwatsubo[1,*]

[1]Department of Neuropathology, Graduate School of Medicine, The University of Tokyo, Hongo 7-3-1, Bunkyo-ku, Tokyo 113-0033, Japan
[2]Department of Pathology, Graduate School of Medicine, The University of Tokyo, Hongo 7-3-1, Bunkyo-ku, Tokyo 113-0033, Japan
[3]Department of Neurochemistry, Graduate School of Medicine, The University of Tokyo, Hongo 7-3-1, Bunkyo-ku, Tokyo 113-0033, Japan
[4]Departments of Bioengineering and Psychiatry and Behavioral Sciences, Stanford University, Stanford, CA 94305, USA
[5]Department of Neurology, Hope Center for Neurological Disorders, Knight Alzheimer's Disease Research Center, Washington University, St. Louis, MO 63110, USA
[6]Co-first author
*Correspondence: iwatsubo@m.u-tokyo.ac.jp
http://dx.doi.org/10.1016/j.celrep.2015.04.017

SUMMARY

In vivo experimental evidence indicates that acute neuronal activation increases Aβ release from presynaptic terminals, whereas long-term effects of chronic synaptic activation on Aβ pathology remain unclear. To address this issue, we adopted optogenetics and transduced stabilized step-function opsin, a channelrhodopsin engineered to elicit a long-lasting neuronal hyperexcitability, into the hippocampal perforant pathway of APP transgenic mice. In vivo microdialysis revealed a ~24% increase in the hippocampal interstitial fluid Aβ42 levels immediately after acute light activation. Five months of chronic optogenetic stimulation increased Aβ burden specifically in the projection area of the perforant pathway (i.e., outer molecular layer of the dentate gyrus) of the stimulated side by ~2.5-fold compared with that in the contralateral side. Epileptic seizures were observed during the course of chronic stimulation, which might have partly contributed to the Aβ pathology. These findings implicate functional abnormalities of specific neuronal circuitry in Aβ pathology and Alzheimer disease.

INTRODUCTION

Aggregation of amyloid β peptides (Aβ) as senile plaques and vascular amyloid is the hallmark pathological change in the brains of patients with Alzheimer disease (AD) (Selkoe et al., 2012). Recent studies using electrical or pharmacological stimulations have shown that Aβ is secreted from neurons in an activity-dependent manner (Kamenetz et al., 2003; Cirrito et al., 2005, 2008). Furthermore, recent human and animal studies using molecular and functional imaging techniques have shown that cortical regions that are most prone to amyloid deposition in aging or AD, as revealed by amyloid positron emission tomography (PET) imaging, correspond to those consisting of a functional network termed default mode network, where basal brain activities at resting state are constantly high (Buckner et al., 2005; Bero et al., 2012). These observations led to an intriguing hypothesis that chronic synaptic hyperactivity is causally related to the deposition of Aβ and linked to the pathogenesis of AD. However, verification of this hypothesis in animal models has not been feasible due to the limitation in methodologies applicable to long-term repetitive experimentations.

Recently, optogenetics has emerged as a revolutionary method that enables the selective control of the activities of a specific population of neurons that are engineered to express channelrhodopsin (CR) (Yizhar et al., 2011). Optogenetics by expressing CR has brought about a groundbreaking advance in the functional analysis of the brain circuitry, including those involved in brain disorders (Tye and Deisseroth, 2012). However, classical CRs, like electrical or pharmacological stimulations, are relatively short acting and have not been suitable for chronic experiments to model neurodegenerative disorders that require long-lasting stimulation for months.

In this study, we adopted the recently developed stabilized step-function opsin (SSFO), taking advantage of its unusual capacity to keep neurons closer to action potential threshold and increasing the probability of spiking to endogenous synaptic inputs as long as for 30 min by a single light stimulation (Yizhar et al., 2011). We demonstrated that chronic activation of a specific neuronal tract augments Aβ pathology within its presynaptic projection area in vivo.

RESULTS

Viral Transduction of SSFO and Optogenetic Activation of Perforant Pathway Neurons in APP Transgenic Mice

To selectively stimulate the cortical projection neurons in the lateral entorhinal cortex (LEC) that project to the hippocampal dentate gyrus (DG) through the perforant pathway, we unilaterally transduced SSFO-enhanced yellow fluorescent protein (EYFP) or EYFP in adeno-associated virus (AAV) vector driven by a CaM kinase II α promoter into the LEC of amyloid β precursor

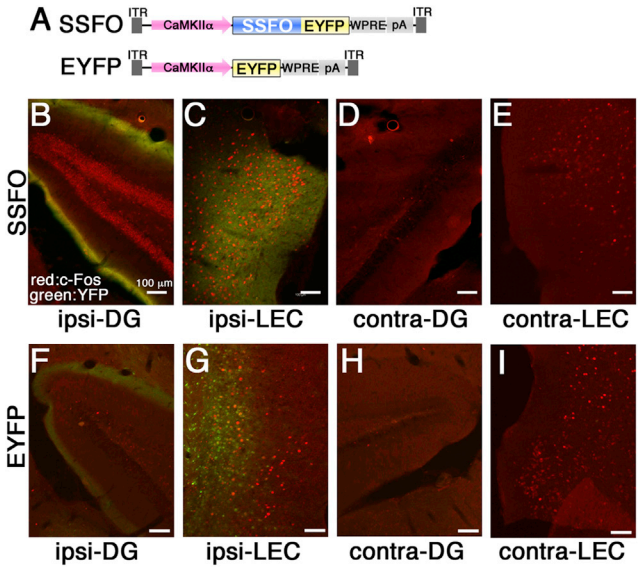

Figure 1. Optogenetic Stimulation Activated Perforant Pathway Neurons

(A) Schematic structures of SSFO-EYFP (SSFO) and EYFP (EYFP) driven under the control of CaMKIIα promoter in an AAV vector are shown. ITR, the inverted terminal repeat sequences; CaMKIIα, Ca^{2+}/calmodulin-dependent protein kinase II alpha (promoter); WPRE, woodchuck hepatitis virus posttranscriptional regulatory element; pA, polyadenylation signal.

(B–I) Immunofluorescence labeling for c-Fos (neuronal activation marker, red) and YFP (virus expression marker, green) of the coronal sections of mice infected with AAV-SSFO (B–E) or AAV-EYFP (F–I). Expression of SSFO or EYFP (green) was observed in perforant pathway neurons of the ipsilateral side of infection, i.e., LEC (ipsi-LEC, C and G) and OML of the DG (ipsi-DG, B and F), but not in those of the contralateral side (contra-DG, D and H, and contra-LEC, E and I). Unilateral optogenetic stimulation increased the levels of c-Fos at ipsilateral DG (B) and LEC (C) (red), specifically in the SSFO-infected mice. Note that non-stimulated LEC neurons show modest levels of basal c-Fos activities (E, G, and I).

protein (APP) Tg mice (A7 line; Yamada et al., 2009; Figure 1A). We also immunostained the brain sections for c-Fos as a marker of neuronal activation. After 1 month of viral infection, we inserted a fiber optic cannula and stimulated infected neurons of the LEC by blue light.

Immunofluorescence labeling of the coronal sections of mice infected with AAV-SSFO-EYFP in the LEC showed protein expression of SSFO fused to EYFP in the outer molecular layer (OML) of the DG (Figure 1B), as well as within the LEC around the injection site (Figures 1C and S1A, low-power view). Ninety minutes after a single optogenetic activation of LEC neurons transduced with SSFO-EYFP, ipsilateral LEC neurons exhibited stronger c-Fos immunoreactivity compared to neurons of the contralateral side (Figures 1C and 1E), with both being stronger than prior to light stimulation (data not shown). Neurons in the ipsilateral DG became c-Fos positive after light stimulation of the LEC, whereas contralateral DG neurons remained almost negative (Figures 1B and 1D). In mice infected with AAV-EYFP in the LEC, LEC neurons of virus-infected or from the contralateral side exhibited moderate c-Fos immunoreactivity at comparable levels (Figures 1G and 1I), and DG neurons were negative

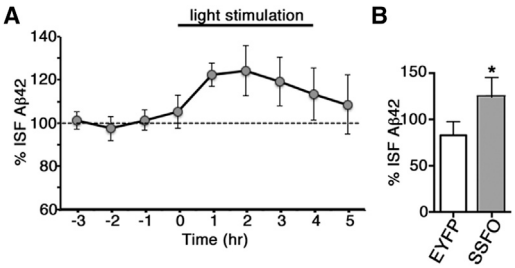

Figure 2. Acute Optogenetic Stimulation of the LEC Increased Aβ42 Levels in the Hippocampus

(A) Average levels of ISF Aβ42 in the hippocampus of APP Tg mice infected with SSFO detected by an in vivo microdialysis technique. Light stimulation (1×/min for 4 hr) increased the ISF level of Aβ42. Mean relative levels of ISF Aβ42 ± SEM (mean of those 1, 2, and 3 hr prior to stimulation as 100%) are indicated (n = 5).

(B) Quantitative analysis of ISF Aβ42 levels at 1 hr of stimulation. ISF level of Aβ42 in the hippocampus of SSFO-infected APP Tg mice was significantly higher than that for mice infected with EYFP (n = 4 [EYFP] and 5 [SSFO], respectively; Student's t test, mean ± SD, *p < 0.05).

for c-Fos on both sides (Figures 1F, 1H, and S1B, low-power view). These results indicate that SSFO-EYFP is optimally transduced to the perforant pathway neurons, which can be activated by light stimulation of the LEC.

Acute Optogenetic Stimulation of the LEC Increased ISF Aβ42 Levels in the Hippocampus

To determine whether the acute optogenetic stimulation of the perforant pathway upregulates Aβ release in vivo, we transduced SSFO-EYFP or EYFP into the LEC neurons of A7 mice and quantitated Aβ42 levels in the interstitial fluid (ISF) of the hippocampus using microdialysis. We perfused artificial cerebrospinal fluid (aCSF) containing 0.15% BSA and collected ISF through a microdialysis probe with 35-kDa molecular weight cutoff membrane inserted into the hippocampus.

We intermittently stimulated LEC neurons of A7 mice infected with SSFO-EYFP or EYFP for 2 s per minute for 240 min. During the initial 60 min of stimulation, light stimulation of A7 mice infected with SSFO-EYFP significantly increased hippocampal ISF Aβ42 levels by 24.3% compared to the average levels 0 to 240 min prior to stimulation, suggesting that optogenetic stimulation effectively enhanced Aβ release in vivo (Figures 2A and 2B). During the subsequent stimulation (from 60 to 240 min), ISF Aβ42 leveled off and gradually decreased with increased variations in Aβ levels among animals. No significant increase in the levels of hippocampal ISF Aβ42 was detected with light stimulation of EYFP-infected A7 mice (Figure 2B).

Effects of Chronic Optogenetic Stimulation of LEC Neurons on Aβ Deposition in the Projection Area of the Hippocampal Perforant Pathway

We then examined whether chronic optogenetic stimulation affects Aβ pathology in the brains of female A7 mice. We carefully examined Aβ pathology throughout the brains, especially in the OML of the DG, where small, diffuse Aβ deposits often form band-like clusters in a variety of APP transgenic mice (Games et al., 1995; Mucke et al., 2000). Since SSFO renders infected

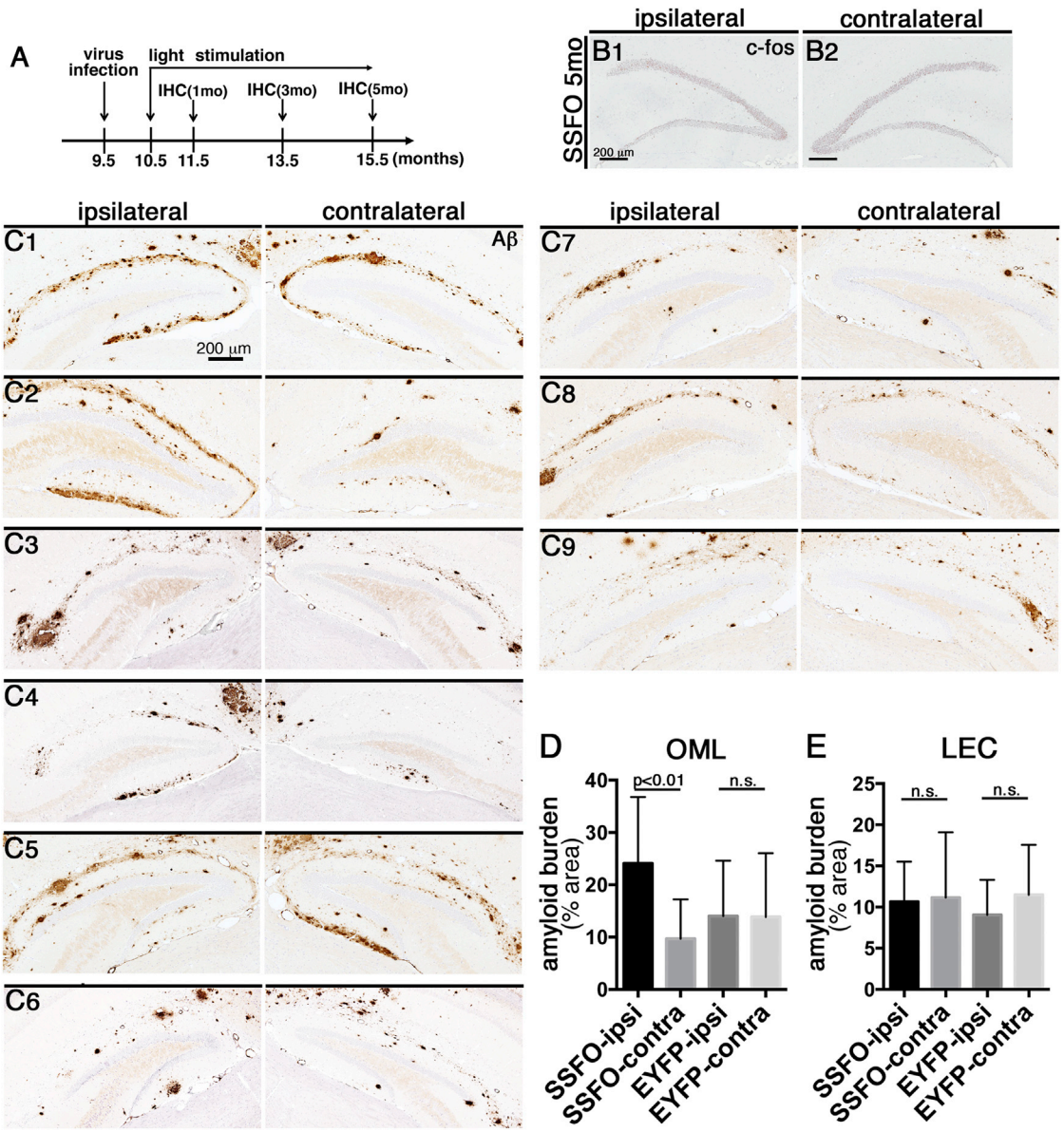

Figure 3. Chronic Optogenetic Stimulation of LEC Neurons Increased Aβ Deposition at the OML of the DG of Ipsilateral Hippocampus

(A) Schematic representation of the experimental timeline. Virus infection was performed at 9.5 months; light stimulation was started at 10.5 months; and immunohistochemical (IHC) analysis was done after 1, 3, or 5 months of light stimulation.

(B) The c-Fos immunoreactivity of the hippocampal DG ipsilateral (left) or contralateral (right) to the light-stimulated side in APP Tg mice stimulated for 5 months is shown.

(C) Aβ depositions in the DG of hippocampus ipsilateral (left) or contralateral (right) to the side of optogenetic stimulation of the LEC for 5 months in APP Tg mice infected with SSFO are shown. Scale bar, 200 μm.

(D) Quantitative analysis shows amyloid burden at the OML of the DG ipsilateral (ipsi) or contralateral (contra) to the side of optogenetic stimulation of the LEC for 5 months in SSFO- or EYFP-infected APP Tg mice.

(E) The ratio of amyloid burden at the ipsilateral/contralateral LEC in SSFO- (left) or EYFP- (right) infected APP Tg mice optogenetically stimulated for 5 months (n = 9 [SSFO] and 10 [EYFP], respectively, in D and E; Student's t test, mean ± SD, $p > 0.05$; n.s., no significant differences).

neurons hyperexcitable for >30 min upon a single 2-s stimulation (Yizhar et al., 2011), we chose a protocol to chronically stimulate the LEC of A7 mice once for 2 s every 24 hr, to periodically increase ISF Aβ42 levels every day, starting at 10.5 months old for 1, 3, and 5 months (Figure 3A).

Immunohistochemistry for c-Fos showed that neurons in the DG of both sides were positive at 1, 3, and 5 months, suggesting that chronic stimulation upregulated expression of immediate early genes on both hemispheres (Figures 3B, S1D, and S1E), whereas no change was observed in EYFP-infected mice

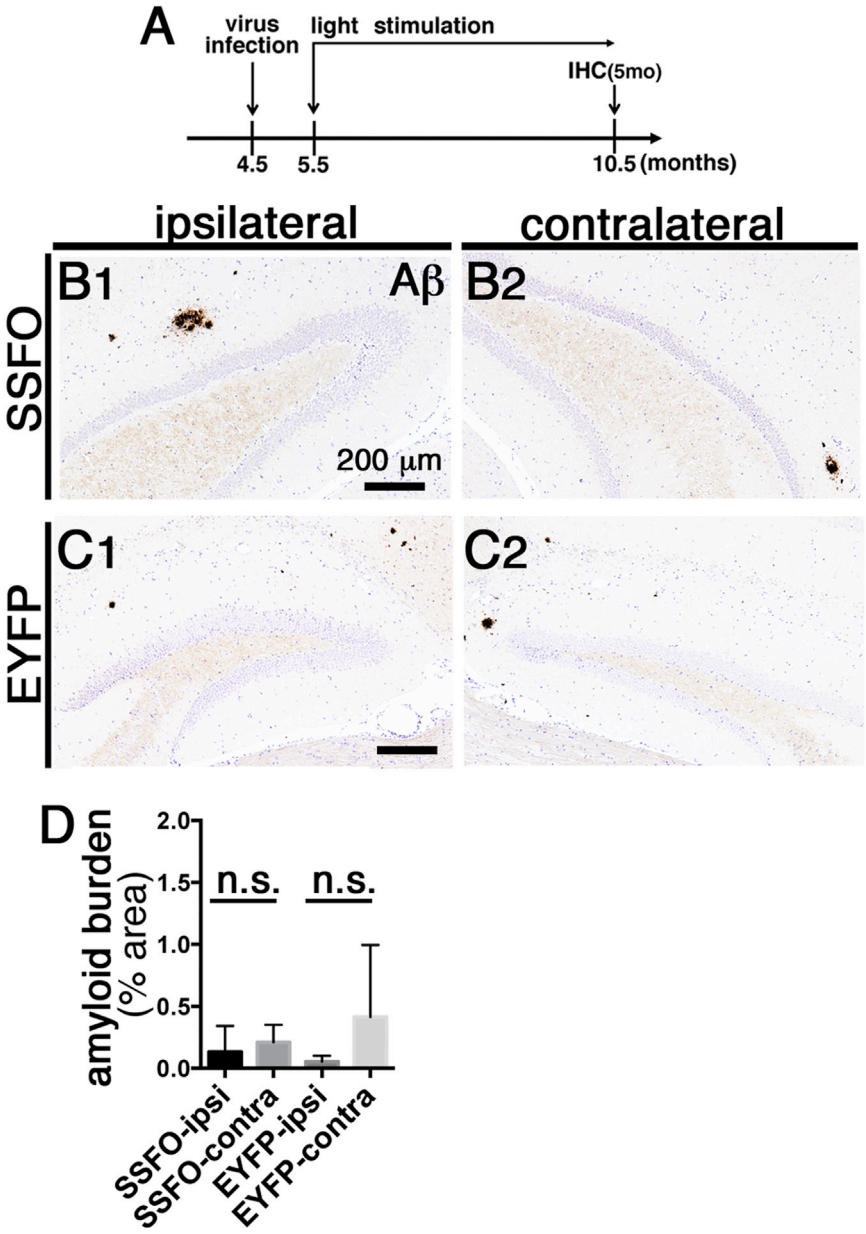

Figure 4. Chronic Optogenetic Stimulation of LEC Neurons, Starting at 5.5 Months Old for 5 Months, Did Not Increase Aβ Deposition

(A) Schematic representation of the experimental timeline. Virus infection was performed at 4.5 months, light stimulation started at 5.5 months, and IHC analysis was done after 5 months of light stimulation.

(B and C) Aβ deposition in the DG of hippocampus ipsilateral (B_1 and C_1) or contralateral (B_2 and C_2) to the side of optogenetic stimulation of the LEC for 5 months in APP Tg mice infected with SSFO (B) or EYFP (C). Scale bar, 200 μm.

(D) Quantitative analysis shows amyloid burden at the OML of the DG ipsilateral (ipsi) or contralateral (contra) to the side of optogenetic stimulation of the LEC in SSFO- or EYFP-infected APP Tg mice (n = 4 [SSFO] or 5 [EYFP], respectively; Student's t test, mean ± SD, $p > 0.05$; n.s., no significant differences).

(Figure S1C). We assessed Aβ deposition by immunohistochemistry and quantitated the percentage of areas covered by Aβ immunoreactivity (Aβ burden) within the OML of the DG by morphometry (Iwatsubo et al., 1994). We also confirmed that all animals expressed detectable levels of SSFO-EYFP or EYFP throughout the perforant pathway by immunohistochemistry for EYFP (Figures S1F and S1G).

APP Tg mice transduced either with AAV-EYFP or AAV-SSFO-EYFP, after 1 month of light stimulation, showed occasional Aβ deposits in the cerebral cortices or hippocampus; however, no differences in histopathology were observed regardless of the type of transduced proteins or stimulation side (Figure S2A), and the Aβ burden was at negligible levels (Figure S2B). EYFP- or SSFO-EYFP-infected mice stimulated for 3 months showed a small amount of Aβ deposits in the OML of the DG as well as in other areas of cerebral cortices; a single animal transduced with SSFO-EYFP exhibited a larger amount of Aβ deposits specifically in the OML of the stimulated side (Figure S2A), although the mean levels of amyloid burden were not significantly different (~0.5%–1.4% in each group, Figure S2C). In mice optogenetically stimulated for 5 months, we observed a significant increase in Aβ deposits in the OML of the stimulated side, compared with that of the contralateral side (Figure 3C), by ~2.5-fold (~24% versus ~10% as amyloid burden, $p = 0.0098$, Figure 3D), whereas amyloid deposition in other areas of the cerebral cortex, including those in the LEC, was present at similar levels on either side (Figure 3E).

Immunohistochemistry for the C terminus of Aβ42 also showed the predominance of Aβ deposits in the OML of the stimulated side (~10.3% versus ~5.9%, $p = 0.022$) in the 15.5-month-old mice transduced with SSFO-EYFP (Figures S3B and S3C). No other apparent pathological changes besides Aβ deposition were observed. Amyloid burden in the OML of mice transduced with EYFP as a control was similar on both sides (~13%), which was lower than that of the stimulated side of SSFO-infected mice (Figures 3D and S3A). We also examined A7 mice at 10.5 months of age optically stimulated for 5 months starting at 5.5 months of age, but did not observe the emergence of premature Aβ deposition (Figures 4B–4D).

To determine whether chronic neuronal activation upregulates production of Aβ, or alternatively it affects the release of Aβ from the presynaptic terminals, we quantitated the levels of Aβ42, sAPPβ, and sAPPα in the ISF recovered from hippocampus by

microdialysis in 7- to 10-month-old A7 mice after chronic stimulation for 3 months. A single optic stimulation in these mice elicited a significant increase in Aβ42 levels (Figures S4A and S4B), whereas those of sAPPβ (Figure S4C) and sAPPα (Figures S4D and S4E) were not altered.

During the course of chronic optogenetic stimulation, epileptic seizures, which appeared to be equivalent to perforant pathway kindling, were observed exclusively and virtually in all SSFO-transduced mice (Figure S2D). Typically, the seizures started after ~5 s of light stimulation as a clonic-tonic generalized convulsion, ceasing within ~2 min. Some animals only showed motor arrest after stimulation, which was sometimes followed by a convulsion. Epileptic seizures were observed exclusively following optical stimulation, did not recur after recovery from a seizure, and were never elicited spontaneously independent of light stimulation. The epileptic phenotype was never observed in the EYFP-transduced mice.

DISCUSSION

In this study, we adopted optogenetics to the experimental activation of a specific neuronal pathway in APP transgenic mice as a model of AD, to examine the causal relationship between synaptic activation and Aβ pathology, and showed the following: (1) chronic optogenetic activation of the hippocampal perforant pathway for up to 5 months of stimulation was feasible based on AAV-mediated transduction and stable protein expression of SSFO, a long-acting CR; (2) augmentation of Aβ pathology, possibly through the chronic increase in Aβ release, was achieved in the presynaptic projection area using SSFO by optogenetics; and (3) our model implicates hyperactivity of a specific projection pathway in the augmentation of Aβ deposition. Our study provides strong support for the notion that functional impairment in neural circuits may underlie Aβ pathology and AD pathogenesis, and further opens up the application of optogenetics in chronic experiments in animal models of neurodegenerative disorders.

The main merit of optogenetic techniques is in the selective control of the activity of neurons by a short-term light stimulation, depending on the functional specificity of the CR, and selectivity in the neuronal populations expressing CR. Accordingly, application of optogenetics in the study of brain disorders has been limited to acute experiments, e.g., selectively controlling activities of a specific subset of neurons involved in functional or behavioral abnormalities in parkinsonism, epilepsy, affective disorders, or addiction, to unravel the neuronal circuits involved in these disorders (Tye and Deisseroth, 2012). Taking advantage of the stability in expression for over several months and performance of SSFO to induce a continuous hyperexcitable state by a single light stimulation, we were able to add an application of optogenetic stimulation to the in vivo modeling of AD pathology by a chronic stimulation paradigm. This was not possible previously with the classical electrical or pharmacological stimulation.

It has been shown previously, using acute electrical or pharmacological stimulation, that Aβ is released from the presynaptic termini into the ISF by an activation-dependent mechanism in the perforant pathway of APP transgenic mice (Cirrito et al., 2005, 2008). Conversely, dissection of the perforant path abolished Aβ deposition in the OML of the DG, implicating the specific involvement of perforant pathway neurons in the formation of Aβ deposits in its terminal zone (Lazarov et al., 2002). Our study has demonstrated that Aβ pathology can be modified by a chronic and intermittent neuronal hyperactivation lasting for 5 months in the presynaptic area of the perforant pathway, linking synaptic activity and Aβ deposition in vivo. Since aggregation of Aβ is a concentration-dependent process, it would be reasonable that an increased supply of soluble Aβ from the presynaptic endings, along with alterations in aggregation and degradation, accelerated the Aβ deposition in the terminal zone of the perforant pathway.

Notably, 5 months of stimulation that started at a young age (i.e., 5.5 months old) did not advance the initiation of Aβ deposition. Because aggregation of Aβ is a seed-induced process (Jarrett and Lansbury, 1993), the initial seed formation that triggers amyloid deposition in APP transgenic mice is dependent on the aging of brain tissues, not only on the Aβ levels in the ISF. It remains to be determined whether chronic neuronal activation upregulates production of Aβ, or alternatively if it affects only the release of Aβ from the presynaptic terminals. Our present observations that levels of Aβ42, but not those of sAPPα or sAPPβ (the latter being the product of β cleavage, a rate-limiting step for Aβ production), were increased in the ISF upon optic activation after chronic stimulation (Figure S4), as well as the lack of changes in immunoreactivities for APP, sAPPβ, sAPPα, and BACE1 in tissue sections of the LEC and DG (data not shown), may support the view that an increase in Aβ release is one of the major mechanisms underlying the activity-dependent Aβ increase.

Our results may be relevant to the observation, in humans and animals, that cortical areas that develop the largest amount of Aβ deposits in aged or AD brains (e.g., posterior cingulate cortex/precuneus/retrosplenial cortex) also have the highest basal rates of metabolic and neural activity measured by glucose PET and functional MRI, which recently was defined as the default mode network that is activated when a person is not performing a specific mental task, i.e., in default state (Buckner et al., 2005; Raichle et al., 2001; Bero et al., 2012). It has been hypothesized that the high level of neural activity in these cortical areas throughout life might make them susceptible to Aβ deposition due to the relationship between synaptic activity and Aβ.

It is noteworthy that our mice developed stimulation-induced epileptic seizures during the course of chronic stimulation. This additional factor, which can be interpreted as perforant pathway kindling, might have enhanced the activity-dependent Aβ release from the presynaptic terminals of the perforant pathway. Recently, the involvement of seizures and latent epileptic activities in the pathogenesis of AD was highlighted (Palop and Mucke, 2009). It has been documented that surgically removed cortical tissues from ~10% of patients with temporal epilepsy exhibited the premature emergence of Aβ deposits, as early as in the fourth decade of life (Mackenzie and Miller, 1994).

While we were able to establish a method to achieve chronic hyperactivation of a specific neuronal pathway using optogenetics, the strength of the neuronal activation might have been more intense compared to those in physiological condition, although the extent of increase in lactate levels in hippocampal ISF after optogenetic activation was considerably milder

(+74% at 30 min after stimulation) (Figure S4F) compared with that upon hyperactivation induced by picrotoxin (+342%) (Yamada et al., 2014). It would be ideal if we were able to control the activity of SSFO-infected neurons at more modest levels for a longer period. This may enable us to determine whether increased synaptic activity at physiological levels, such as occurs in chronically activated neural networks, might also modify Aβ pathology as well as subsequent failures in the network activities.

EXPERIMENTAL PROCEDURES

Animals

Transgenic mice (line A7) that overexpress human APP695 harboring K670N, M671L (Swedish), and T714I (Austrian) familial AD mutations in neurons under the control of Thy1.2 promoter were used (Yamada et al., 2009). C57BL/6J mice were purchased from Charles River Laboratories. All animals were maintained on food and water with a 12-hr light-dark cycle. All experiments were approved by the Institutional Animal Care and Use Committee of the Graduate Schol of Medicine at the University of Tokyo.

Construction of AAV Vectors and Transfer to Mouse Brains

AAV was produced in a baculovirus/sf9 system. In brief, a DNA fragment encoding SSFO-EYFP was ligated to CaMKIIα promoter and inserted into an AAV vector for amplification in baculovirus. The resultant vector was transformed into DH10BAC and the expression cassette was transposed into bacmid and transfected into Sf9 cells to produce baculovirus. The resultant baculovirus was co-infected with an AAV1-packaging baculovirus into Sf9 cells at an MOI of two. AAV was purified on AVB sepharose (GE Healthcare). The AAV fraction was concentrated by ultrafiltration using Amicon Ultra 100K-15 (Millipore).

Then, 1.0 μl AAV solution (10^{12}–10^{13} genome copies/ml) was stereotaxically injected into mouse brains through a glass capillary (100-μm tip diameter) inserted into the LEC. More details on our methods are included in the Supplemental Experimental Procedures.

Optical Stimulation

After 4 weeks of AAV infection, mice were again stereotaxically inserted with a fiber optic cannula into the LEC. In chronic optical stimulation experiments, female A7 mice (9.5 months old) were infected with AAV coding for SSFO-EYFP or EYFP, and, after 1 month of incubation, mice were optically stimulated for 2 s every 24 hr (starting at the age of 10.5 months) for 1, 3, or 5 months by blue light (473 nm, 4 mW). In each group, 6–8 mice were stimulated for 1 or 3 months and ~10 mice were used for a 5-month optic stimulation. In acute stimulation experiments, optic stimulation for 2 s (at 4 mW) was performed each minute for 4 hr, starting after 6 hr of ISF sampling by microdialysis. More details on our methods are included in the Supplemental Experimental Procedures.

In Vivo Microdialysis Combined with Acute Optical Stimulation and ELISA Quantitation of Aβ

A microdialysis cannula was inserted stereotaxically into the hippocampal area, filled with aCSF containing 0.15% BSA, and set with a dialysis probe of molecular weight cutoff at ~35 or ~1,000 kDa. The aCSF was circulated at the rate of 1.0 μl/min and sampling was started after 2 hr, with mice in a free-moving state. After recovery of brain ISFs, an equal volume of 1M guanidine hydrochloride was added and incubated for 30 min to solubilize and monomerize the recovered Aβ. Levels of Aβ42 in ISF were quantitated by Human/Rat β Amyloid (42) ELISA kit (Wako Pure Chemicals Industries) as described previously (Iwatsubo et al., 1994). More details on our methods are included in the Supplemental Experimental Procedures.

Immunohistochemistry and Morphometry

Mouse brains perfused with 4% paraformaldehyde (PFA) were cut into 30-μm-thick cryosections and analyzed by immunofluorescence for expression of c-Fos and SSFO-EYFP. Immunohistochemical and morphometric analyses of Aβ deposition were performed on paraffin-embedded, 4-μm-thick coronal sections of mouse brains stained with a mouse monoclonal anti-Aβ antibody 82E1 or anti-Aβ(38-42). Quantitation of Aβ burden was conducted using ImageJ software. Four to five consecutive sections, 100 μm apart at the level of the largest section of hippocampus, were examined and the mean level of Aβ burden was calculated for each animal. The outermost one-third of the molecular layer throughout the entire extent of the DG was examined. More details on our methods are included in the Supplemental Experimental Procedures.

Statistical Analyses

Quantitative data were analyzed statistically by Student's t test or ANOVA using Prism 6 (GraphPad).

SUPPLEMENTAL INFORMATION

Supplemental Information includes Supplemental Experimental Procedures and four figures and can be found with this article online at http://dx.doi.org/10.1016/j.celrep.2015.04.017.

AUTHOR CONTRIBUTIONS

K.Y., T.H., T.W., H.O., M.F., H.B., J.R.C., D.M.H., K.D., and T.I. designed the research. K.Y., Z.T., T.H., T.W., Y.N., and T.I. performed the research. O.Y., L.E.F., and K.D. contributed unpublished reagents/analytic tools. K.Y., Z.T., T.H., T.W., and T.I. analyzed the data. T.H., D.M.H., and T.I. wrote the paper.

ACKNOWLEDGMENTS

We thank Drs. Ryuta Koyama and Yuji Ikegaya of The University of Tokyo and our lab members for helpful discussions. This work was supported by Grants-in-Aid for Scientific Research on Innovative Areas "Foundation of Synapse and Neurocircuit Pathology"; Comprehensive Brain Science Network of the Ministry of Education, Culture, Sports, Science and Technology; and by grants from Core Research for Evolutional Science and Technology, Japan.

Received: October 31, 2014
Revised: March 5, 2015
Accepted: April 7, 2015
Published: April 30, 2015

REFERENCES

Bero, A.W., Bauer, A.Q., Stewart, F.R., White, B.R., Cirrito, J.R., Raichle, M.E., Culver, J.P., and Holtzman, D.M. (2012). Bidirectional relationship between functional connectivity and amyloid-β deposition in mouse brain. J. Neurosci. *32*, 4334–4340.

Buckner, R.L., Snyder, A.Z., Shannon, B.J., LaRossa, G., Sachs, R., Fotenos, A.F., Sheline, Y.I., Klunk, W.E., Mathis, C.A., Morris, J.C., and Mintun, M.A. (2005). Molecular, structural, and functional characterization of Alzheimer's disease: evidence for a relationship between default activity, amyloid, and memory. J. Neurosci. *25*, 7709–7717.

Cirrito, J.R., Yamada, K.A., Finn, M.B., Sloviter, R.S., Bales, K.R., May, P.C., Schoepp, D.D., Paul, S.M., Mennerick, S., and Holtzman, D.M. (2005). Synaptic activity regulates interstitial fluid amyloid-β levels in vivo. Neuron *48*, 913–922.

Cirrito, J.R., Kang, J.E., Lee, J., Stewart, F.R., Verges, D.K., Silverio, L.M., Bu, G., Mennerick, S., and Holtzman, D.M. (2008). Endocytosis is required for synaptic activity-dependent release of amyloid-β in vivo. Neuron *58*, 42–51.

Games, D., Adams, D., Alessandrini, R., Barbour, R., Berthelette, P., Blackwell, C., Carr, T., Clemens, J., Donaldson, T., Gillespie, F., et al. (1995). Alzheimer-type neuropathology in transgenic mice overexpressing V717F β-amyloid precursor protein. Nature *373*, 523–527.

Iwatsubo, T., Odaka, A., Suzuki, N., Mizusawa, H., Nukina, N., and Ihara, Y. (1994). Visualization of A β 42(43) and Aβ 40 in senile plaques with end-specific

Aβ monoclonals: evidence that an initially deposited species is Aβ 42(43). Neuron *13*, 45–53.

Jarrett, J.T., and Lansbury, P.T., Jr. (1993). Seeding "one-dimensional crystallization" of amyloid: a pathogenic mechanism in Alzheimer's disease and scrapie? Cell *73*, 1055–1058.

Kamenetz, F., Tomita, T., Hsieh, H., Seabrook, G., Borchelt, D., Iwatsubo, T., Sisodia, S., and Malinow, R. (2003). APP processing and synaptic function. Neuron *37*, 925–937.

Lazarov, O., Lee, M., Peterson, D.A., and Sisodia, S.S. (2002). Evidence that synaptically released β-amyloid accumulates as extracellular deposits in the hippocampus of transgenic mice. J. Neurosci. *22*, 9785–9793.

Mackenzie, I.R., and Miller, L.A. (1994). Senile plaques in temporal lobe epilepsy. Acta Neuropathol. *87*, 504–510.

Mucke, L., Masliah, E., Yu, G.Q., Mallory, M., Rockenstein, E.M., Tatsuno, G., Hu, K., Kholodenko, D., Johnson-Wood, K., and McConlogue, L. (2000). High-level neuronal expression of abeta 1-42 in wild-type human amyloid protein precursor transgenic mice: synaptotoxicity without plaque formation. J. Neurosci. *20*, 4050–4058.

Palop, J.J., and Mucke, L. (2009). Epilepsy and cognitive impairments in Alzheimer disease. Arch. Neurol. *66*, 435–440.

Raichle, M.E., MacLeod, A.M., Snyder, A.Z., Powers, W.J., Gusnard, D.A., and Shulman, G.L. (2001). A default mode of brain function. Proc. Natl. Acad. Sci. USA *98*, 676–682.

Selkoe, D., Mandelkow, E., and Holtzman, D. (2012). Deciphering Alzheimer disease. Cold Spring Harb. Perspect. Med. *2*, a011460.

Tye, K.M., and Deisseroth, K. (2012). Optogenetic investigation of neural circuits underlying brain disease in animal models. Nat. Rev. Neurosci. *13*, 251–266.

Yamada, K., Yabuki, C., Seubert, P., Schenk, D., Hori, Y., Ohtsuki, S., Terasaki, T., Hashimoto, T., and Iwatsubo, T. (2009). Abeta immunotherapy: intracerebral sequestration of Abeta by an anti-Abeta monoclonal antibody 266 with high affinity to soluble Abeta. J. Neurosci. *29*, 11393–11398.

Yamada, K., Holth, J.K., Liao, F., Stewart, F.R., Mahan, T.E., Jiang, H., Cirrito, J.R., Patel, T.K., Hochgräfe, K., Mandelkow, E.M., and Holtzman, D.M. (2014). Neuronal activity regulates extracellular tau in vivo. J. Exp. Med. *211*, 387–393.

Yizhar, O., Fenno, L.E., Prigge, M., Schneider, F., Davidson, T.J., O'Shea, D.J., Sohal, V.S., Goshen, I., Finkelstein, J., Paz, J.T., et al. (2011). Neocortical excitation/inhibition balance in information processing and social dysfunction. Nature *477*, 171–178.